Pergamon

Int. J. Solids Structures Vol. 32, No. 17/18, pp. 2813–2828, 1995
Elsevier Science Ltd
Printed in Great Britain
0020-7683/95 $9.50 + .00

0020-7683(94)00296-7

A HIGH-SPEED DIGITAL IMAGING SYSTEM FOR RECORDING NON-REPETITIVE TRANSIENT EVENTS

C. P. BURGER, R. CHONA, S. K. KHANNA and M. R. THOMAS
Department of Mechanical Engineering, Texas A&M University, College Station, TX 77843-3123, U.S.A.

(*Received* 3 *February* 1994)

Abstract—A high-speed digital imaging system employing electronic controls and standard optical elements has been developed. A cavity-dumped argon laser is used to provide very short duration monochromatic light pulses with short interpulse times, while an acousto-optic deflector provides spatial separation of each image. Electronic solid-state imaging is accomplished with charge injection device cameras. Full frame images (512 × 512 pixels) of the actual light intensity variations in the imaged object are digitally recorded to a resolution of 256 gray levels using a frame grabber and a host computer. This system has applications in the study of high-speed phenomena, such as dynamic fracture, impact mechanics and fluid flow.

INTRODUCTION

High-speed dynamic phenomena are encountered in many areas of science and engineering. A greater research effort is needed to understand and develop applications of dynamic phenomena in the areas of impact mechanics, fracture mechanics, high-speed machining, fluid flow and materials science. In this context a dynamic even is considered one in which the phenomenon changes very rapidly with time and is generally non-periodic. Thus, the most important tool for conducting research on dynamic phenomena is a high-speed imaging system that can record images of the event at predetermined, discrete time intervals.

Several high-speed imaging systems have been built by scientific researchers, others are commercially available. Such systems include: the multiple spark Cranz–Schardin camera developed by, among others, Cranz and Schardin (1929), Riley and Dally (1969) and Field (1982); the rotating mirror camera after Field (1982); and the image convertor camera after Garfield and Riches (1990). However, these cameras are often expensive and are difficult to assemble in a short time in a university laboratory because of the complexities involved. In addition, each of these imaging systems has its own drawbacks that make its performance less than ideal for some high-speed experimental mechanics imaging needs. For example, the Cranz Schardin and the rotating mirror cameras use photographic film as the recording medium, which involves a non-linear development process and results in the actual light intensity variations being modulated during processing. The image convertor cameras use electrons impinging on a phosphor screen for generating an image, which is also a non-linear process. Therefore, there is a need for a high-speed electronic imaging system using a solid-state imaging device, such as the charge couple device (CCD) or the charge injection device (CID) camera, which record the actual light intensity levels in digital format. This allows the image to be stored in a computer and later analyzed using the many available image processing techniques.

The development of an electronic imaging system that can record the light intensity variations without introducing any non-linearities is important when studying real life engineering materials as opposed to model materials. This is because optical mechanics studies on actual material systems (e.g. ceramics and ceramic composites) will not yield a large number of cycles of light intensity variations over the field of observation because the material deformations are generally small. Hence, being able to use the intensity variations between the peaks and valleys of the intensity distribution is essential. The goal of the newly developed system described in this paper is to obtain a digital record of the actual light

Table 1. Requirements of a high-speed imaging system

Characteristic of system	Requirement
Exposure time per image	Less than 50 ns
Interframe time	2–500 μs (programmable)
Recording medium	Solid-state imager
Light intensity variation record	Actual/definable variations
Pixel format	Square
Resolution	15 line-pairs mm^{-1}
Image distortion	Less than 1%
Minimum number of images per event sequence	4
Moving parts	None
Operation and maintenance	Relatively easy

intensity variations due to non-repetitive transient events, at high framing rates and using very short exposure times.

Some examples of the application of high-speed imaging are in studying crack propagation and wave propagation in materials. Cracks propagate in ceramics at a speed of about 2000 m s^{-1}. Hence, to capture an instantaneous image of the crack tip region without blurring of the image, an imaging system is needed which has an exposure time of about 50 ns and a framing rate of about 500,000 frames s^{-1} (or an interframe time of 2 μs). In order to capture events at such short interframe times, separate CID cameras must be used to record each successive image, since the time required to read out one full frame is about 30 ms. Therefore, both spatial and temporal separation must be obtained for each image.

In the new digital imaging system that has been developed, an acousto-optic (AO) deflector has been used to obtain the necessary spatial separation. An AO deflector, or Bragg cell, diffracts the incident laser beam into zero and first order beams. The angle through which the first order beam is diffracted depends on the acoustic frequency, and thus this diffraction angle can be altered and the spatial separation attained through simple input frequency shifting with no mechanically moving parts. Hendley *et al.* (1975) used an AO deflector to obtain spatial separation of light beams in an attempt to mimic the Cranz–Schardin camera; excepting this, no application of an AO deflector for high-speed electronic imaging has come to the attention of the authors up to this point. The temporal separation of the images in the current system is obtained through the pulsing capabilities of a cavity-dumped laser. The spatial separation of the laser beam due to the AO deflector coupled with the programmable time delays and very short pulse durations of the light pulses emitted by a cavity-dumped laser form the basis of the present high-speed imaging system.

REQUIREMENTS OF THE HIGH-SPEED IMAGING SYSTEM

The basic requirements for any high-speed imaging system are: the ability to separate spatially the light beam at different times; an image recording medium which is sensitive to the attainable light intensity levels; a recording medium that does not introduce non-linearities in the recorded image; a short duration exposure time to capture sharp pictures of rapidly occurring events; resolution of the image that is sufficiently high to allow spatial separation of details in the image; minimal image distortion; relative ease of operation and synchronization with the event to be recorded; and minimal cost. Table 1 lists some of the quantitative requirements of a high speed imaging system.

AVAILABLE HIGH-SPEED CAMERAS

Several high-speed imaging systems are currently available. Some available systems that are widely used by the mechanics community are briefly described below and discussed with regard to their capabilities and drawbacks.

Multiple spark Cranz–Schardin camera

This camera, shown in Fig. 1(a), has multiple electric spark units, each having its own energy source and spark gap. A single trigger initiates the sequential firing of the array of spark gaps. The time between firing of subsequent spark gaps is controlled by changing the inductance in the LC loop of each spark gap. Each spark provides a high intensity light flash which lasts for about 0.5 μs. These light flashes are used to illuminate the object and to shutter the camera. The light passes through a system of lenses and the image is recorded on a photographic film that is sensitive to blue light.

This camera has been used extensively for fracture and impact studies, especially using the optical technique of photoelasticity. Synchronization of the event with the camera is easily achieved by using a number of sequenced electronic circuits as shown by Riley and Dally (1969). When the event occurs the camera fires after a preset delay and 16–20 frames are recorded, depending on the number of spark gaps provided in the design of the camera. However, since these spark gaps are spread in an array around the optical axis of the camera, inevitably there is parallax. Also, very high electric voltages are present in the LCR circuits of each spark gap, and thus extreme caution is necessary on the part of the user. Finally, the images are recorded on photographic film which introduces distortions in the actual light intensity distribution during the nonlinear development process.

Rotating mirror camera

This camera uses a mirror that spins at very high speeds [Fig. 1(b)]. The mirror is driven by a gas turbine and rotation speeds up to 20,000 rev s^{-1} can be attained. The mirror is made of beryllium, which is a very light weight, high strength material. Good light reflection properties are obtained by coating the beryllium substrate with aluminum that is further protected by a vapour-deposited quartz coating. In this camera the film is held stationary and the event is first imaged onto the rotating mirror which then reflects the light through framing lenses and slits onto the film.

Synchronization of the event with the light source is difficult for a rotating mirror camera utilizing film over a 60° arc. In such an arrangement, the event has to be synchronized with the light source, and thus it is difficult to capture the image properly. The triggering is done by sensing the position of the mirror and then passing this signal into the delay units which trigger the event and the light source. On the other hand, if the film is spread over a full 360°, it is easier to synchronize since the light remains on while the event is taking place. The problems associated with using film as a recording medium are, however, still present.

Image convertor camera

The working principle and camera construction of this system are shown schematically in Fig. 1(c) following Garfield and Riches (1990). The incident light from the specimen falls on the photocathode, which generates electrons proportional to the intensity of incident light at each point. The light image is thus converted into an electron image at the photocathode and is later converted back into a light image at the phosphor screen. Shuttering of the electron image is effected by a combination of three mesh electrodes. Electrode 3 is held at a fixed potential in order to establish the field conditions within the image section required for tube focusing. Electrode 1 is held at a fixed potential and defines the reference potential about which electrode 2 and the photocathode was switched in sequence in order to shutter the beam on and off. The deflector plates direct the image onto the desired position on the phosphor screen. By shuttering and proper deflection of the electron beam at discrete intervals, several images can be obtained on the screen. These images can then be transferred onto film or a video camera.

This type of camera is fully electronic and can be triggered directly from the occurrence of the event. It can be operated under low light levels, as the electron tube gives an effective light gain. The camera is portable and can be useful for on-site inspections. The picture quality of the image convertor camera, however, is not as good as that of the rotating mirror camera, but is better than the Cranz–Schardin camera. On the negative side, depending on the type of phosphor screen, the emission peaks at a particular wavelength of light and falls

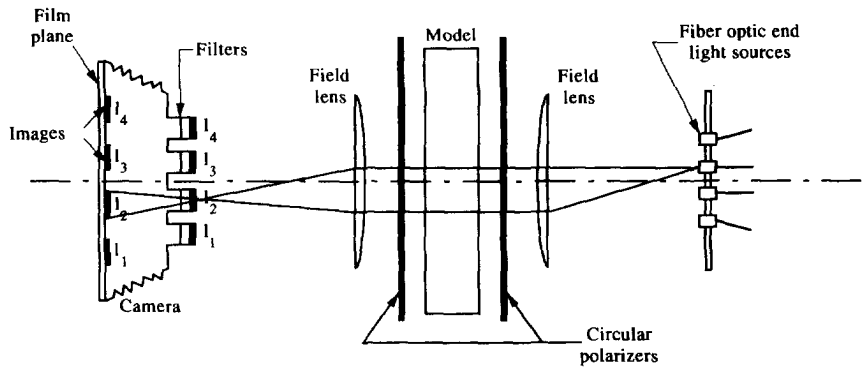

(a) Multiple Spark Cranz-Schardin Camera

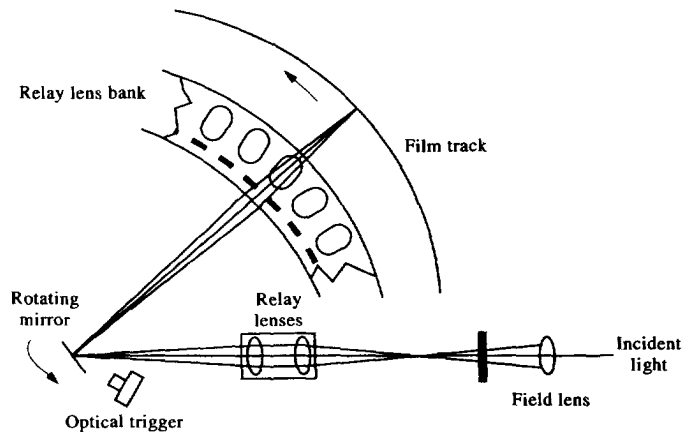

(b) Rotating Mirror Camera

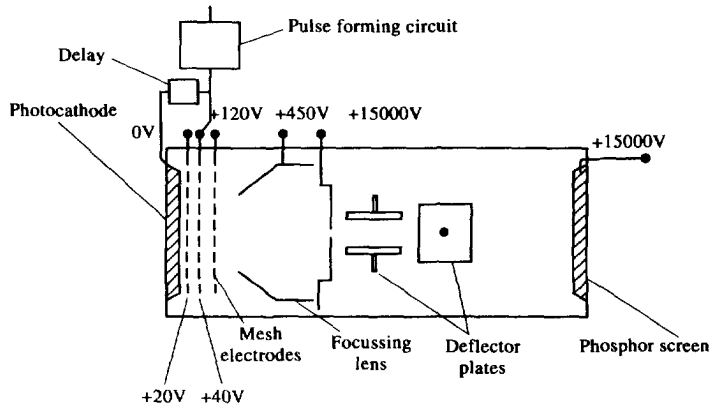

(c) Image convertor camera

Fig. 1. Schematic diagram of three existing high-speed imaging systems.

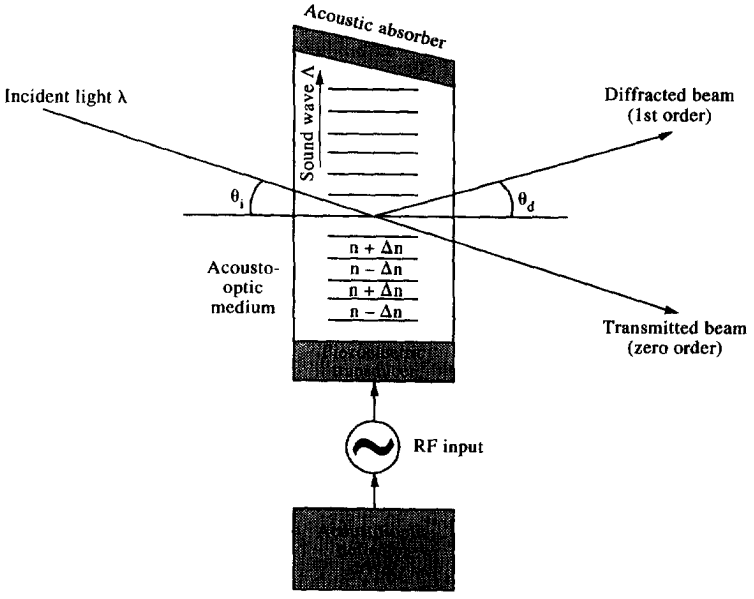

Fig. 2. Schematic diagram of acousto-optic diffraction of light using an acousto-optic deflector.

off rapidly on either side of the peak. The intensity on the phosphor screen decays non-linearly after being bombarded by the electrons from the photocathode. Also, the phosphor screen luminance is a linear function of the photocathode illuminance only over a small region and is non-linear otherwise. Thus, the intensity variations recorded become distorted from the actual light intensity distribution at the object.

PHILOSOPHY OF THE NEW HIGH-SPEED IMAGING SYSTEM

The new high-speed imaging system attains a level of performance that is unattainable with any of the existing systems. It incorporates a laser with a cavity dumper to obtain the short duration pulse of light needed to image the specimen or event being studied. This allows the object to be illuminated for the required interval and for successive flashes to occur within the necessary period. The spatial separation is obtained with a Bragg cell, which is driven by a staircase frequency input to obtain the spatial separation with time that is necessary for each image. After being manipulated by the proper optics, a single image is recorded on each of the four CID cameras in the current system. It is assumed that the principles of operation of cavity-dumped lasers and digital cameras are fairly well known, however, the operation of an AO deflector may not be as widely understood. Given the fact that the Bragg cell is central to the configuration proposed for the present system, its theory of operation is discussed further in the following section.

ACOUSTO-OPTIC DEFLECTOR

An AO deflector, or Bragg cell, is a device that produces diffraction of incident light due to its interaction with sound waves. A Bragg cell consists of an optically transparent crystal which is driven by a piezoelectric device, causing sound waves to travel through the medium. As sound propagates through this optically transparent medium, typically a quartz crystal, it produces a periodic variation of the refractive index due to a pressure disturbance that includes regions of compression and rarefaction in the crystal. This effect, shown schematically in Fig. 2, can be considered to generate a diffraction grating that can move or change at the speed of sound (Das and Decusatis, 1991). A laser beam passing through

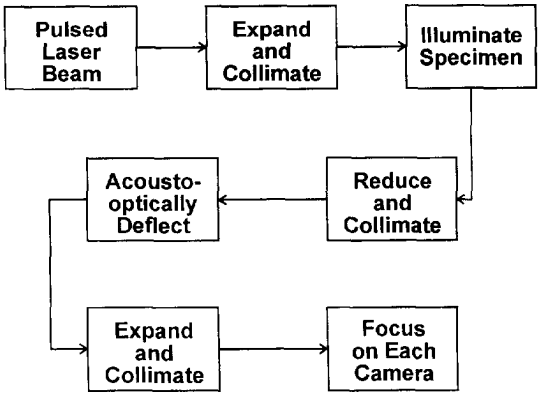

Fig. 3. Schematic block diagram of the layout of the imaging system using scheme 1.

this grating will diffract into several diffraction orders. By proper design of the Bragg cell, the first order diffraction beam can have the highest diffraction efficiency. The diffraction angle of the first order beam is dependent on the acoustic frequency of the driving signal; thus, by changing this frequency, the first order diffraction spot can be moved quickly and efficiently with no moving mechanical parts.

The temporary "diffraction grating" generated in the AO medium may be produced by standing or stationary waves, or by travelling acoustic waves such as those used in the current application. For both types of waves, the Bragg condition in which the most light is diffracted into the first order beam is reached when the following equation is satisfied

$$2\Lambda \sin \theta_i = \lambda,$$

where Λ is the wavelength of the sound wave travelling through the AO deflector, θ_i is the Bragg angle and λ is the wavelength of the incident light.

AO deflectors are used in many different applications, the most common of which are bar-code readers at supermarket checkouts. More scientific applications include radio-frequency spectrum analyzers, laser cavity dumpers, and ultraviolet and infrared spectrophotometers (Das and Decusatis, 1991). For the current application, the Bragg cell satisfies the function of producing spatial separation of the images with a switching time of approximately 2 μs.

NEW HIGH-SPEED IMAGING SYSTEM

Optical schemes

Two basic schemes were considered for this high-speed imaging system. The first concept allows a collimated beam to illuminate the same region of the specimen each time and then sends the beam containing image information through the Bragg cell. The second idea uses the Bragg cell to deflect the light beam before it enters the specimen, so that the incident light illuminates the specimen at slightly different locations. Each method has its advantages and disadvantages, which are discussed below for the case of transmission through a transparent specimen.

The first method, shown schematically in Fig. 3, starts with a pulsed laser beam which is expanded and collimated and then passes through the specimen. This image is then reduced in size and collimated in order for it to pass through the small vertical aperture of the AO deflector. As the beam passes through the Bragg cell, it is deflected according to the input frequency from the AO driver. This small beam is again expanded and collimated before being focused onto its appropriate camera. This method has the advantage of allowing each camera to view the same region of the specimen, since the light beam is not

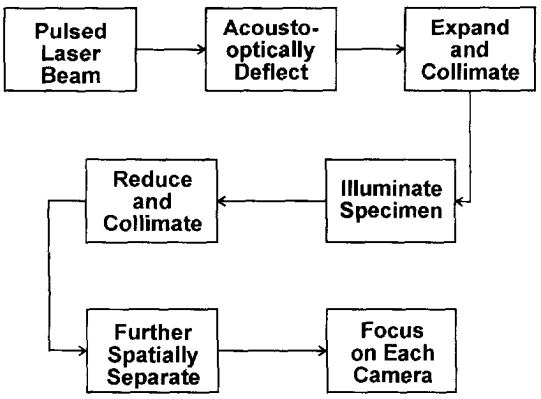

Fig. 4. Schematic block diagram of the layout of the imaging system using scheme 2.

diffracted until after it has passed through the specimen. However, it does require more optical elements, which can reduce the quality of the image somewhat.

The second scheme, shown in Fig. 4, involves sending the pulsed laser beam through the AO deflector prior to illumination of the specimen, followed by expansion and collimation. This beam is then sent through the specimen, after which it must be further spatially separated to accommodate the cameras. The beam is then focused onto the appropriate camera. The main advantages of this concept are its relative simplicity and the fact that, for very rapid crack propagation for example, it might be desirable to have a light beam which moves across the specimen as the area of interest moves, rather than imaging the entire area of the specimen at all times. A limitation to this method, however, is that the spatial separation is very difficult to obtain, since the expansion and collimation necessary immediately after the Bragg cell tend to bring the light back to the central optical axis, thus diminishing the separation obtained from the AO deflector. Although this problem will be addressed in the future, the first method is the one that has been pursued further at the present time.

Experimental set-up

The basic experimental set-up for the high-speed imaging system is shown in Fig. 5. The light source for the system was a Spectra-Physics Model 164 argon ion laser, continuously emitting light at 514.5 nm wavelength. A Spectra-Physics Model 344 cavity dumper allows for either continuous or single pulsing of the laser, with pulses ranging from 10 to 30 ns in width at frequencies of up to 10 MHz. The present imaging system uses externally triggered pulses at 25 ns pulse width for each image.

The pulses are directed by mirrors to the first expansion/collimation pair of lenses, as shown in Fig. 5. For this set-up, convex lens 1 is a 50 mm diameter/38 mm focal length biconvex lens and convex lens 2 is a 50 mm diameter/500 mm focal length biconvex lens. This set-up increases the beam diameter to approximately 25 mm. The central portion of the laser beam (about 10 mm in diameter) was used to ensure more uniform intensity distribution, and this was achieved with a simple iris diaphragm aperture. Thus, the light beam which passes through the specimen is about 10 mm in diameter. Although the planned use and major benefit of this system are to capture high-speed dynamic events, static specimens are currently being used as the system is being developed and evaluated. The specimens used for the current discussion are a square test grid and photoelastic specimens placed between circular polarizers. Two convex lenses are used after the specimen to reduce the beam size from 10 mm to 5 mm. Convex lens 3 is a 50 mm diameter/200 mm focal length biconvex lens and convex lens 4 is a 50 mm diameter/100 mm focal length biconvex lens.

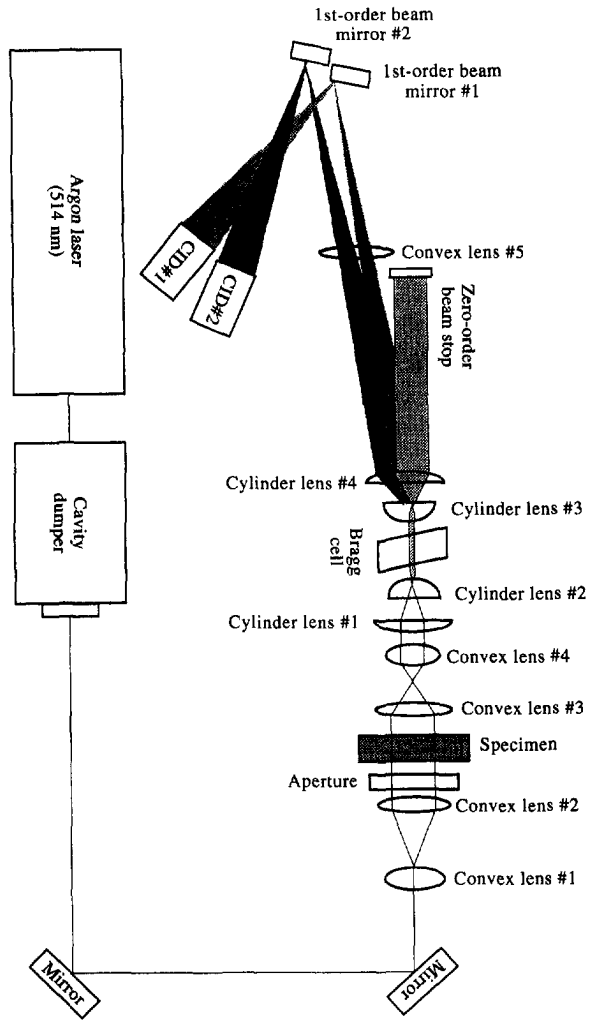

Fig. 5. Schematic diagram of the optical layout of the high-speed imaging system.

As shown in Fig. 5, the image is passed through a set of cylinder lenses both in front of and behind the Bragg cell. This was found to be necessary for two reasons. First, the vertical aperture (the one perpendicular to the direction of travel of both the light and the acoustic wave) is just less than 1.5 mm; thus the beam size must be reduced considerably in order to travel through the Bragg cell. However, using an ordinary set of convex lenses to reduce the beam to a spot of less than 1.5 mm diameter was found to be inadequate because the beam dimension in the horizontal direction is small, resulting in low resolution of the Bragg cell.

This is better understood from the governing expression for the number of resolvable spots, N, in the plane of the Bragg cell. N is given by

$$N = \Delta f \tau,$$

where Δf is the frequency bandwidth of the Bragg cell and τ is the time it takes the acoustic waves to cross the optical aperture. For a particular Bragg cell, Δf is fixed and τ can be varied. If τ is small, as above, then N is low which limits the amount of information that can be transmitted by the Bragg cell. In our case $\Delta f = 100$ MHz and $\tau = 0.35$ μs (for a 1.5 mm spot size), resulting in a value of $N = 35$ which is the number of resolvable spots per millimeter. Thus, for transmitting a line which is 0.15 mm wide in the object plane and

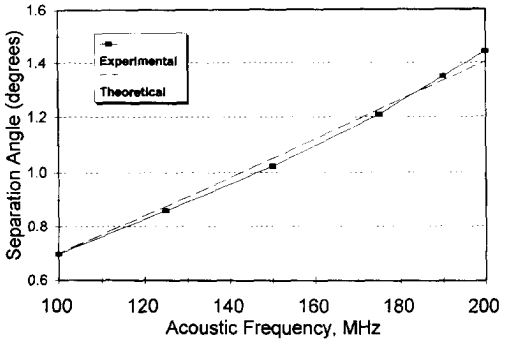

Fig. 6. Optical deflection of the first order diffracted beam as a function of the input driving frequency of the acousto-optic deflector.

0.022 mm wide in the plane of the Bragg cell, the minimum value of N should be 45, which is higher than that obtained with a 1.5 mm circular spot. This results in blurring of the line.

The resolution of the Bragg cell can be improved by using a spot of light which is less than or equal to the height of the optical aperture in the vertical direction and as long as possible in the horizontal direction. This can be achieved by the use of appropriate cylinder lenses. In this study, a set of cylinder lenses was used with their axes oriented in the same direction as the direction of travel of the acoustic wave. The image was thus reduced in size vertically but not horizontally, and therefore passed through the Bragg cell cleanly. The spot of light transmitted through the Bragg cell was 1.5 mm high and 5 mm wide. This resulted in a resolution of $N = 117$. Also the horizontal blurring was not seen when this type of image travelled through the Bragg cell because the resolution of the spot was increased due to the higher beam dimension in the horizontal direction. A second set of cylinder lenses was oriented in the same manner and served to make the spot circular again.

In this set-up, cylinder lenses 1 and 4 are 50 mm diameter/100 mm focal length lenses, while cylinder lenses 2 and 3 are 13 mm diameter/25 mm focal length lenses. The Bragg cell, which is mounted on a rotary positioner, was oriented at the Bragg angle with respect to the incident beam, so that the light was most efficiently diffracted into the first order beam. The Bragg cell used was a Model ADM-150 Acousto-Optic Deflector-Modulator manufactured by IntraAction Corporation, and uses a tellurium oxide (TeO_2) crystal. The separation angle obtained as a function of the input driving frequency for this AO deflector is shown in Fig. 6. The diffraction efficiency over the acoustic frequency range of 100–200 MHz was nearly constant at about 60% of light being transmitted into the first order beam and dropped significantly outside this range.

The light emerging from the Bragg cell consisted of two beams. The zero order beam was always present in the same location and direction and a beam stop was necessary to block out the undesirable light from the zero order beam. The first order beam was the one of interest here, because it could be extinguished by turning off power to the Bragg cell and moved by changing the input voltages into the Bragg cell driver, i.e. changing the acoustic frequency. Convex lens 5 (50 mm diameter/750 mm focal length) was used for two reasons. First, it improved the focus of the image. Second, it allowed the use of plane mirrors to give greater separation of the beams as follows. Mirror 1 was placed near the focal point of the convex lens and adjusted to allow the first image beam to strike just near the edge of the mirror, as shown in Fig. 5. Mirror 2 was then placed immediately behind the first mirror, and when the acoustic frequency was changed the diffracted spot moved sufficiently so that it would fall on the second mirror. The small angle between the plane of mirror 1 and mirror 2 allowed a greater spatial separation to be obtained between images 1 and 2.

Finally, the charge-integration device cameras were placed at twice the focal length from convex lens 5 to obtain focused images approximately 5 mm in diameter. The cameras used were CIDTEC Model 2250 CID cameras, one master and one slave. While the

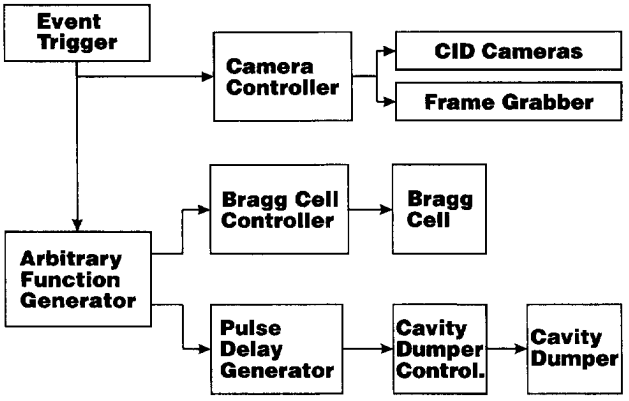

Fig. 7. Block diagram showing the flow of electrical signals between various components of the high-speed imaging system.

preceding discussion has involved only two images, it should be noted that this general set-up allows for at least four and, with minor refinements, up to eight spatially separated images to be obtained of a single event.

Signals and timing

A schematic signal flow diagram for the high-speed imaging system is shown in Fig. 7. The event triggers an external signal (e.g. by breaking a wire as the crack begins to propagate). For the static case investigated in this study, the external trigger was generated with a single pulse from a Wavetek Function Generator. This trigger signal was sent to two locations: the camera controller circuitry and the arbitrary function generator. The custom-built camera controller circuitry synchronizes the external signal with the camera-generated clock and picture sync signals, generates the appropriate timing signals, prepares the frame

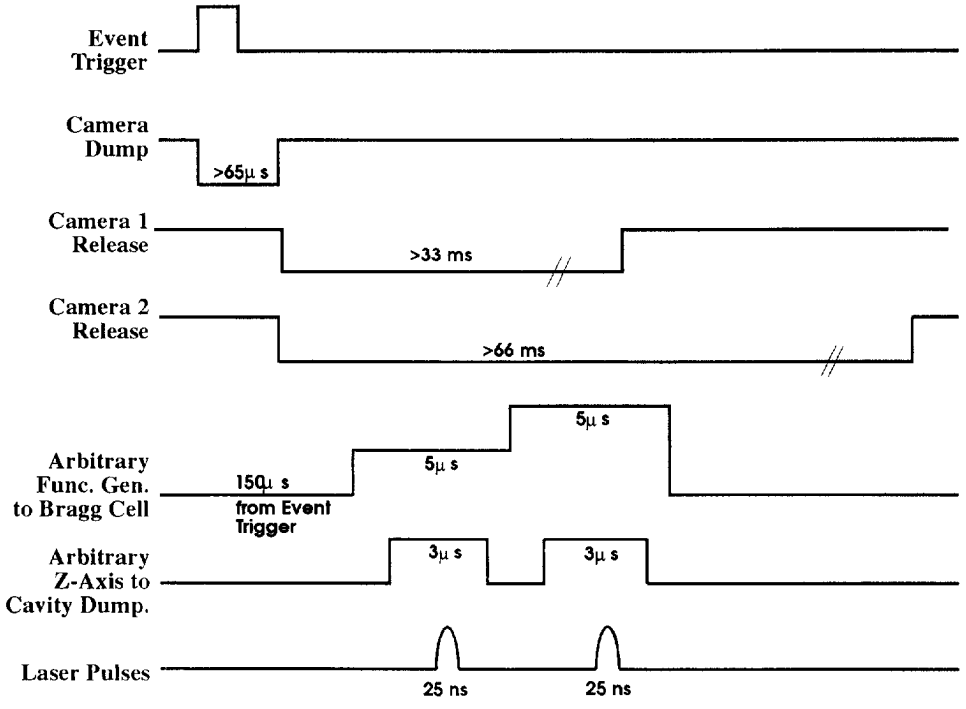

Fig. 8. Schematic diagram showing the relative timings of the various signals.

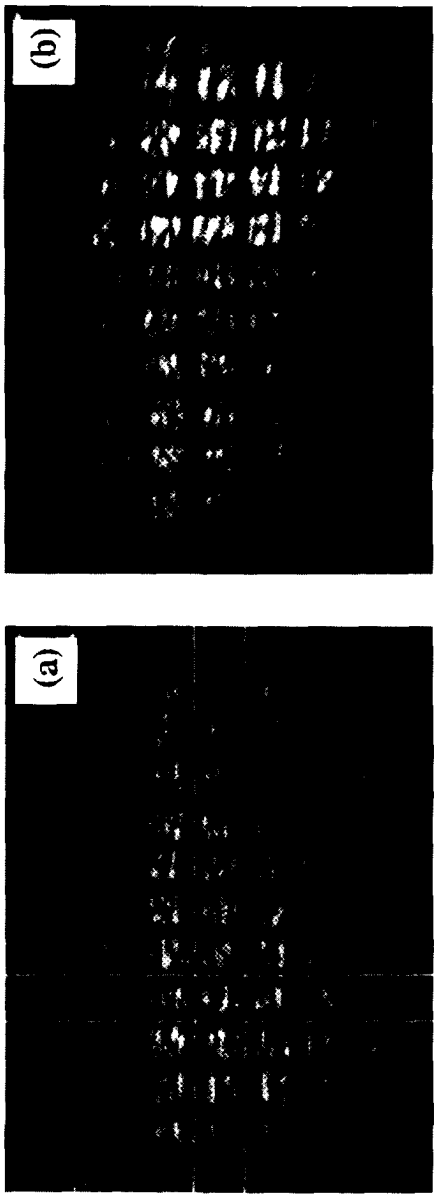

Fig. 9. A 1 mm square test grid imaged with: (a) CID camera 1; and (b) CID camera 2, using a laser pulse of 25 ns duration.

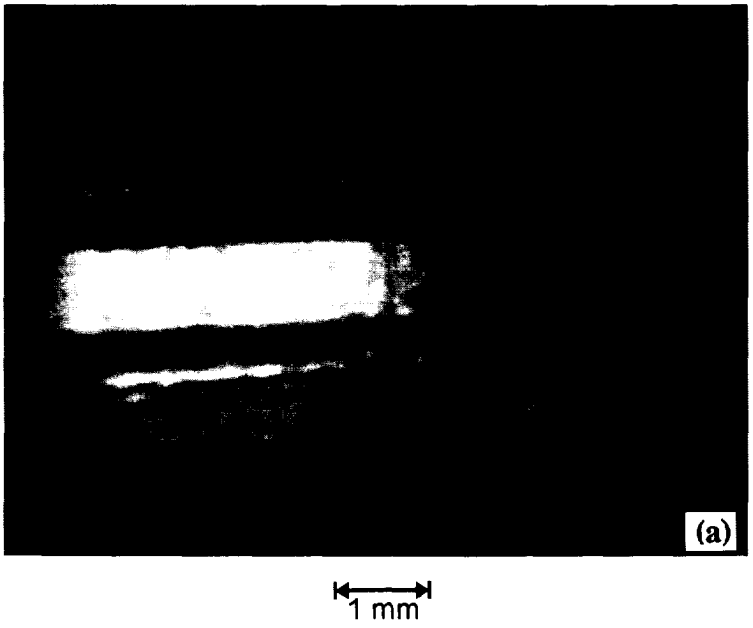

Fig. 10. (a) Isochromatic fringe pattern around a crack under external tensile load; (b) contrast enhanced isochromatics.

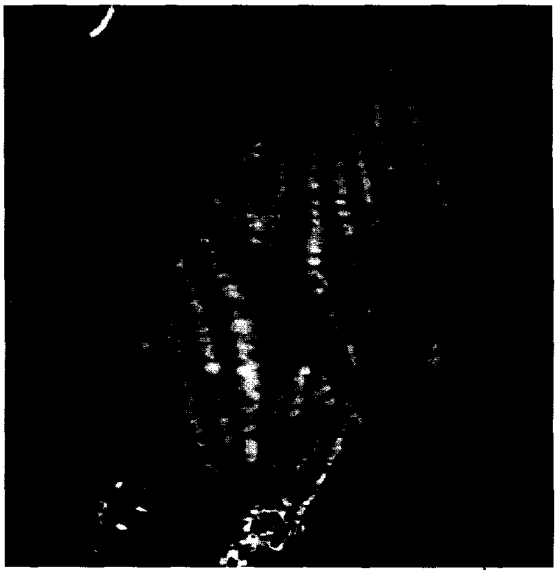

Fig. 11. Isochromatic fringe pattern in a polycarbonate disk under compression obtained by using a 25 ns wide laser pulse.

grabber to receive the images and sends signals to clear, or dump, the charge on the camera registers, reset the frame on each camera and to release the video signals to the frame grabber. The frame grabber, which receives the analog video signal from each camera and converts it to a digital 8 bit value (for 256 gray levels), currently consists of two 4MEG Model 10 I/O cards. These will soon be replaced by one 4MEG Model 12 card with multiplexer capabilities, which will allow up to 12 input channels. These 4MEG frame grabbers and the image processing software used, called 4MIP, are manufactured by Epix, Inc.

The external event trigger was also sent to the arbitrary function generator, as shown in Fig. 7. This equipment sends the staircase voltage signal to the Bragg cell controller, which changes the acoustic frequency of the Bragg cell to give the proper predetermined deflection of each image. This arbitrary function generator, the Krohn-Hite Model 5920, also sends a signal to the double pulse generator. The double pulse generator then sends two short pulses to the cavity dumper controller, which triggers the cavity dumper to release a pair of laser pulses.

The timing diagram for the major signals of the system is shown in Fig. 8, which is not drawn to scale, as indicated by the time durations noted on the signals. As mentioned above, the occurrence of the event sends trigger signals to the cameras to dump their current information or the charge on the solid-state array. The rising edge of the dump signal forces the release (also called inject/inhibit, or I/I) signals low, which tells the cameras to continue integrating, or build up charge, for any light that is falling on their sensors. Thus, it is extremely important not only to perform the imaging sequences in the dark, but also to ensure that no leakage light from the laser beam falls onto the face of the CIDs. After a preset amount of time (about 150 μs), the arbitrary function generator produced a staircase voltage signal. The voltages were set in order to place each image on one CID, in this case at 1 and 2 V. On a separate but synchronized channel (called the Z-axis), the arbitrary function generator produces a pulse which was used to trigger the double pulse generator, as shown in Fig. 8. This produced laser light pulses which fell just within the staircase voltage signals a short time later. The I/I signals, meanwhile, were held low for at least one frame time (33 ms), with each being released in sequence at one-frame time intervals to allow the frame grabber time to process the data. This was possible due to the unique feature of the CID cameras which allows them to retain the charge that is built up over time without loss or bleed down. Thus, images with exposure times of 10–30 ns at a few microseconds interframe time could be captured and held on CID cameras for downloading using standard frame grabbers which operated at conventional video frame transfer rates of 33 ms per frame.

HIGH-SPEED SYSTEM DIGITAL IMAGES

As stated above, different specimens were imaged in this first evaluation stage. The first specimen was a square test grid. Two identical images of the grid were recorded on each CID camera as shown in Fig 9(a,b). The small difference in contrast apparent in the two pictures is due to the limitation of currently using two frame grabber boards, with each board having its own blackness and contrast level potentiometer adjustments. The square grid was used to check for any distortions in the image. It should be noted that the lines are straight and perpendicular, as can be seen with the aid of the white lines drawn through the middle of the grid lines. Also, the oval shape of the image is due to the very small aperture that was used in producing these images, since it shows the area of the solid-state array which was not exposed to the pulse as black and thus verifies that the image illumination is due to the laser pulses rather than to stray light.

The second specimen used was a single edge notch fracture specimen under external tensile loading. This specimen was made out of a photoelastic material PSM1 and was placed between two circular polarizers. Two identical images of the photoelastic fringe pattern around the crack tip were recorded one on each CID camera, with an interframe time of 5 μs and an exposure time of 25 ns. However, it may be mentioned that a variable interframe time can be chosen for any experiment. Only one frame is shown in Fig. 10(a).

Figure 10(b) shows the image after contrast enhancement using image processing methods. The third specimen was a polycarbonate disk under compression, placed between two circular polarizers. Again identical images of the stationary isochromatic fringe patterns were recorded on each of the CID cameras; however, only one image is shown in Fig. 11.

SUMMARY AND CLOSURE

A high-speed electronic imaging system has been developed using pulsed laser light, an AO deflector and solid-state imaging devices. A collimated laser beam is used to interrogate an object under external loading, and the AO deflector has been used to deflect this laser beam at preselected intervals to the appropriate electronic imaging device. The deflection of the laser beam can be achieved in a time of about 1 μs. Hence this camera has a potential for attaining framing rates of 1,000,000 frames s^{-1}. However, in the present research we have used a framing rate of 200,000 frames s^{-1}, with the exposure time for each frame being 120 ns. At present the above described system has been evaluated using static specimens, e.g. a transparent specimen with a black square grid inscribed in it and photoelastic specimens under external loading, placed between two circular polarizers. A solid-state, charge injection imaging device records the actual light intensity variations due to the presence of external loads on the specimen and stores them digitally to a resolution of 256 gray levels. Imaging of high speed dynamic events is within the capabilities of this system since very short exposures and very short interframe times are easily obtainable. Dynamic imaging is currently under investigation. Further improvement in the clarity of the images is also underway. This will allow for many more applications in the use of optical techniques and high-speed digital imaging to study the fracture, impact and effect of harsh environments during the general characterization of modern engineering materials.

REFERENCES

Cranz, C. and Schardin, H. (1929). Kinematographic auf ruhendem film and mit extrem hofer bildfrequenz. *Z. Phys.* **56,** 147.

Das, P. K. and Decusatis, C. M. (1991). *Acousto-optic Signal Processing: Fundamentals and Applications.* Artech House, Boston, Massachusetts.

Field, J. E. (1982). High speed photography: techniques and applications, *Opt. Engng* **21,** 709–713.

Garfield, B. R. and Riches, M. J. (1990). A new programmable image convertor framing camera. In *Proceedings of the 19th International Congress on High Speed Photography and Photonics, SPIE* Vol. 1538, pp. 290–298.

Hendley, D. R., Turner, J. L. and Taylor, C. E. (1975). A hybrid system for dynamic photoelasticity. *Exp. Mech.* **15,** 289–294.

Riley, W. F. and Dally, J. W. (Aug. 1969). Recording dynamic fringe patterns with a Cranz–Schardin camera. *Exp. Mech.* **9,** 27N–33N.